Effect of hydrophilic nanoclay on morphology, thermal and mechanical properties of polylactic acid/ polycaprolactone/ oil palm mesocarp fiber biocomposites

Chern Chiet **Eng**[1], Nor Azowa **Ibrahim**[*1], Norhazlin **Zainuddin**[1], Hidayah **Ariffin**[2], Wan Md. Zin **Wan Yunus**[3], Yoon Yee **Then**[1]

[1]Department of Chemistry, Faculty of Science,
University Putra Malaysia, Serdang, Malaysia

[2]Department of Bioprocess Technology, Faculty of Biotechnology and Biomolecular Sciences, University Putra Malaysia, Serdang, Malaysia

[3]Chemistry Department, Centre for Defence Foundation Studies,
National Defence University of Malaysia, Malaysia

*Corresponding author's phone: +603-89466802/6602

E-mail: norazowa@upm.edu.my

Date Received 22nd June 2013
Date Revised 20th November 2013
Date Accepted 27th November 2013

ABSTRACT

The effect of addition of hydrophilic nanoclay on polylactic Acid (PLA)/polycaprolactone (PCL)/oil palm mesocarp fiber (OPMF) biocomposites were investigated. The composites were prepared by melt blending technique and the composites were characterized by X-ray Diffraction (XRD), Fourier Transform Infrared Spectroscopy (FT-IR), Thermogvavimetric Analysis (TGA), Scanning Electron Microscopy (SEM) and Transmission Electron Microscopy (TEM). FT-IR spectra indicate that there is no major peak shifting or formation of new peak in the composites spectra. Intercalated types of PLA/PCL/clay nanocomposites were confirmed by XRD and TEM results. Based on mechanical properties results, PLA/PCL/OPMF/clay bionanocomposites shows better tensile

strength and elongation at break than PLA/PCL/OPMF biocomposites. TGA results show that the presence of clay increases the thermal stability of the bionanocomposites. SEM micrographs revealed that PLA/PCL/OPMF biocomposites consists of cavity indicated poor fiber/matrix adhesion while micrographs of PLA/PCL/OPMF/clay bionanocomposites show better fiber/matrix adhesion as no cavity present at facture surfaces .

Keywords: Bionanocomposites, Biodegradable Polymers, Clay, Natural Fiber

1.0 INTRODUCTION

The oil palm (Elaeis guineensis) originates from South Africa which grows well in all tropical areas of the world and it has become one of the main industrial crops. Malaysian palm oil industry has grown tremendously over the last 25 years and becomes world's leading producer and exporter of palm oil [1]. For every kg of palm oil produced, approximately 4kg of dry biomass is produced, excluding palm oil mill effluent (POME). In 2010, the amount of mesocarp fiber available is 10.80 Mt/year [2]. Therefore, there are huge amount of fiber that can be utilized instead been discard as waste. Traditionally, the mesocarp fiber is mixed with kernel shell and being utilized as solid fuel to generate electricity for the mill. Mesocarp fiber is an elongated cellulose material with 30-50 mm length [3]. The fiber consists of 21.3% of cellulose, 31.9% of hemicelluloses and 26.9% lignin [4]. The tensile strength and Young's modulus of mesocarp fiber are 80 MPa and 500 MPa respectively while the elongation at break is 17% [5].

Natural fiber as reinforcement filler in polymer composites has received increasing attention to researchers as natural fibers have many significant advantages over synthetic fibers. They are environmentally friendly, fully biodegradable, abundantly available, renewable, cheap and have low density [6]. However, there are some disadvantages such as poor wetability, incompatibility with some polymeric matrices and high moisture adsorption

which restrict their usage in polymer composites [7]. Therefore, compatibilizer is needed to improve fiber matrix adhesion. Ibrahim et al [8] incorporate kenaf bast short fiber into PLA with triacetin as compatibilizer r which show improvement in tensile properties and also better adhesion between fiber and matrix.

Polylactic acid (PLA) is biodegradable polymer with good mechanical properties, thermal plasticity and biocompactibility. However, PLA is a comparatively brittle and stiff polymer with low deformation at break. Therefore, modification of PLA is needed in order to compete with other flexible polymers such as polypropylene or polyethylene [9]. Polycaprolactone (PCL) is flexible semi-crystalline biodegradable polymer with low melting point and exceptional blend-compatibility. High flexibility PCL can be considered as a good plasticizer for PLA compared to low molecular weight plasticizers as it does not migrate to the surface of the blended samples and the physical properties cannot be debased [10]. Hoidy et al incorporate octadecylamine-montmorillonite (ODA-MMT) and fatty hydroxamic acid-montmorillonite (FHA-MMT) in PLA/PCL blend and the results revealed that addition of clay improve mechanical properties and also thermal stability of the blends [11].

Bionanocomposites are hybrid nanocomposites involving a naturally occurring polymer (biopolymer) in combination with an inorganic moiety, and showing at least one dimension on the nanometer scale [12]. Kord incorporate nanoclay to the HDPE/rice husk system show increment of tensile strength, tensile modulus, storage modulus and loss modulus. It was found that the composites containing 2 phc (parts per hundred contents) of the nanoclay had the best morphology with intercalated structures. The addition of nanoclay to the rice husk flour reinforced HDPE composite increased crystallization temperature, crystallization enthalpy and crystallinity level [13].

Recently, many studies been conducted by academic or industrial researcher on biodegradable polymer in order to replace conventional non-biodegradable polymer which

cause major drawback to the environment. However, the cost of biodegradable polymer is comparatively higher than petrochemical based non-biodegradable polymer which limits its application. The incorporation of cheap natural fibers such as oil palm mesocarp fibers as reinforcement filler into biodegradable polymer is an alternative to reduce its cost. However, poor wettability, incompatibility with some polymer matrices and high moisture absorption by the fibers limits the uses of natural fibers as reinforcement filler in polymer composites. Therefore, addition of nanoclay is needed to improve interfacial adhesion between fiber and matrix.

The objective of this paper is to investigate the effect of addition hydrophilic nanoclay as compatibilizer in PLA/PCL/OPMF biocomposites by melt intercalation. Various characterization techniques such as X-ray Diffraction (XRD), Fourier Transform Infrared Spectroscopy (FTIR), Themogravimetric Analysis (TGA), Scanning Electron Microscopy (SEM) and Transmission Electron Microscopy (TEM) were used to study the effect of addition of nanoclay on the properties of PLA/PCL/OPMF biocomposites.

2.0 EXPERIMENTAL

2.1 Materials

All reactions were carried out by using reagent grade chemicals (>98% purity) which without further purification. The hydrophilic nanoclay **(**Nanomer® PGV) was purchased from Sigma-Aldrich and used as received. Polylactide Resin 4060D was supplied by NatureWorks while Polycaprolactone (CAPA 650) was supplied by Solvay Caprolactone. Oil palm mesocarp fibers were obtained from Felda Palm Ind. Sdn Bhd., Serting Hilir.

2.2 Preparation of PLA/PCL/Clay Nanocomposites and PLA/PCL/OPMF/Clay Bionanocomposites

The composites was prepared by melt blending technique with the composition of PLA and PCL kept constant at 85 wt% and 15 wt% respectively in blend while the clay and OPMF content varies from 1 wt% to 7 wt% (for PLA/PCL/clay nanocomposites) and 0% to 30% (for PLA/PCL/OPMF biocomposites and PLA/PCL/OPMF/clay bionanocomposites). PLA, PCL, clay and OPMF were manually premixed in a container and fed into Brabender Plastograph EC at 170°C with rotor speed of 50 rpm for 10 minutes. The products were then compression moulded into sheets of 1mm thickness by an electrically heated hydraulic press with a force of 1500 kN at 160°C for 10 minutes. The sample sheets were then used for further characterization.

2.3 Fourier Transform Infrared Spectroscopy (FTIR)

Perkin Elmer Spectrum 100 series spectrometer equipped with attenuated total reflectance (ATR) were used to determine the functional groups and types of the bonding of the samples with the infrared spectra was recorded in the range of frequency of 280 to 4000cm^{-1} with the resolution of 4cm^{-1} and number of scan is 16 scan.

2.4 X-ray Diffraction (XRD)

X-Ray diffraction measurement to determine the d-spacing of the clay was carried out by using X'PERT PRO PW3040 where Cu Kα (λ=1.5406Å) beam operated at 40mA and 45kV with the data recorded in 2θ range of 2° to 10° using the scan rate of 2°/min.

2.5 Transmission Electron Microscope (TEM)

The transmission electron micrographs of the thin layer of the nanocomposites were recorded by Hitachi H-7100 TEM which operated at an accelerating voltage of 100 kV. The thin layer of samples was prepared by using a Reichert Jung Ultracut E microtome equipped with cryo-sectioning unit whereas the samples were sliced into thin layer of about 90 nm by a diamond knife cooled at -120°C with liquefied nitrogen.

2.6 Tensile Properties

Tensile properties were measured with Instron machine model 4301, with grip attachment distance of 45 mm. Load of 1.0 kN was applied at constant crosshead speed of 5 mm min^{-1}. Data was processed with computerized Instron (Software series 9, national instruments GPIB PC2/2a and NI-488.2). Test specimen were prepared and stamped in accordance to ASTM D638 dumbbell parameters. Sample thickness was measure with Mitutoyo Digimatic Indicator, type IDF-112, having measuring accuracy of ± 0.001 mm.

2.7 Themogravimetric Analysis (TGA)

Perkin Elmer TGA7 was used for thermogravimetic analysis of samples where the mass of samples about 15mg and were heated from 35°C to 800°C with the heating rate of 10°C/min. Nitrogen gas was pumped with the flow rate of 20ml/min in order to let the analysis carry out in nitrogen atmosphere.

2.8 Scanning Electron Microscopy (SEM)

The surface morphology of fracture surfaces was observed with scanning electron microscope JEOL JSM-6400 with the samples were sputter coated with gold using Bio-rad coating system before viewing.

3.0 RESULTS AND DISCUSSION

3.1 PLA/PCL/Clay Nanocomposites

3.1.1 Fourier Transform Infrared Spectroscopy (FTIR)

FTIR spectra of PLA/PCL blends, clay and PLA/PCL/clay nanocomposites are shown in Figure 1. The presence of broad band at 3611.28 cm^{-1} for clay shows that the presence of free water molecule vibration as H-O-H stretching of water molecules present in the interlayer region of clay which indicates that nanoclay is hydrophilic. Band at 1635.83 cm^{-1} correspond to OH deformation of water [14]. Clay exhibits peak correspond to O-H stretching (3402.54 cm^{-1}), Si-O stretching (982.78 cm^{-1}) and Si-O bending (406.15 cm^{-1}) respectively.

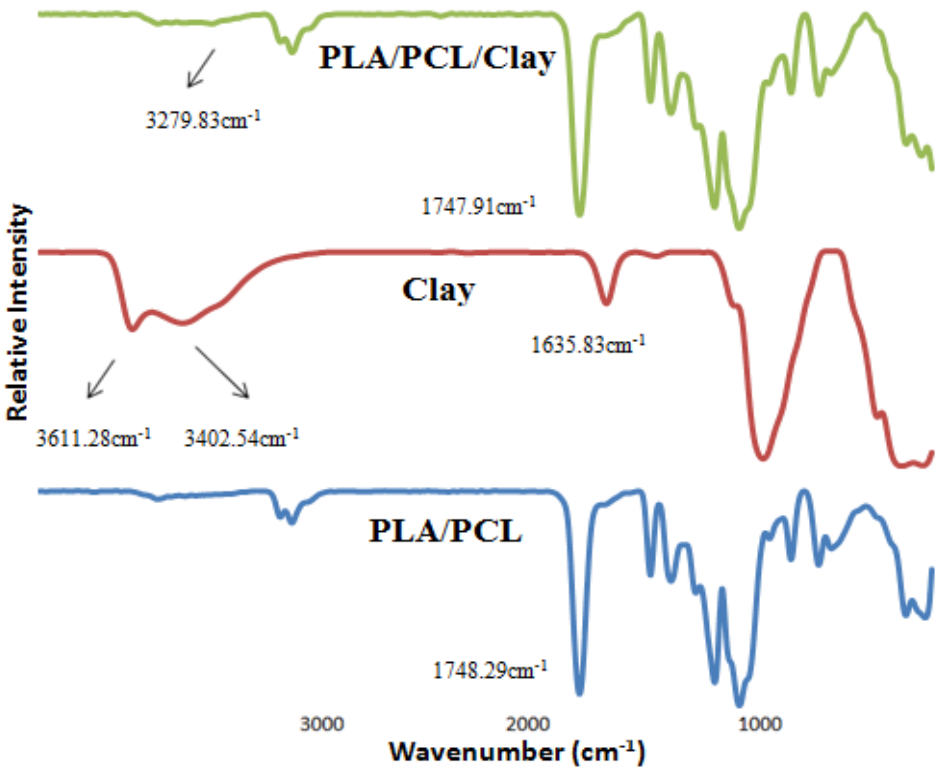

Figure 1: FTIR spectra of PLA/PCL blends, nanoclay and PLA/PCL/clay nanocomposites

FTIR spectra of PLA/PCL and PLA/PCL/clay composites exhibited strong absorbance peak around 1748 cm^{-1} which correspond to the vibration of carbonyl group, C=O

stretching. Peak at 3279.83 cm^{-1} for PLA/PCL/clay composites show the presence of clay in composites. The Si-O stretching peaks appear in the spectrum which indicated the present of clay in the composites. There is no strong interaction among PLA, PCL and clay as no major peak shifting or formation of new peak in the composites spectra.

3.1.2 X-ray Diffraction (XRD) Analysis

The XRD pattern of clay and PLA/PCL/clay composites at different clay loading illustrated at Figure 2. The basal spacing of clay increase from 1.461 nm **(**6.043°**)** to 1.532 nm (5.765**°**), 1.564 nm **(**5.645°) and 1.584 nm **(**5.575°) when 3 wt%, 5 wt% and 7 wt% of clay added into polymer blends respectively. Due to low clay content in composites, the **b**asal spacing of composites with clay loading of 1 wt% could not be detected. All basal spacing of clay and PLA/PCL clay composites are summarized at Table 1.

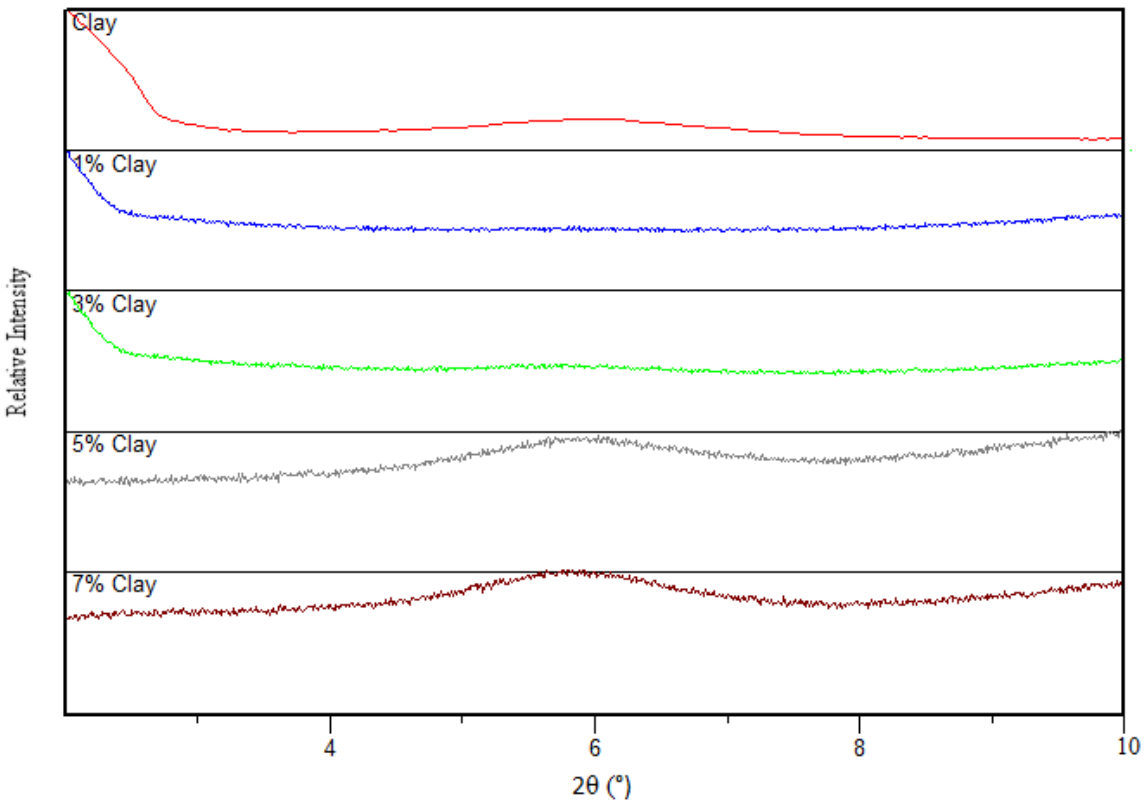

Figure 2: XRD patterns of clay and PLA/PCL composites at different clay loadings

Table 1: Basal spacing of PLA/PCL composites at various clay loadings

Sample	2θ (°)	Basal spacing (nm)
Clay	6.043	1.461
PLA/PCL/ 1wt% Clay	-	-
PLA/PCL/ 3wt% Clay	5.765	1.532
PLA/PCL/ 5wt% Clay	5.645	1.564
PLA/PCL/ 7wt% Clay	5.575	1.584

The increase of the basal spacing of the composites compared to the corresponding neat clay indicated that the PLA/PCL chains were intercalated into the clay matrix during melt intercalation. The peak of clay present in the composites confirms the formation of nanocomposites.

3.1.3 Transmission Electron Microscope (TEM)

The TEM micrograph of PLA/PCL/ 1 wt% clay is shown in Figure 3. The dark area represents the intercalated clay layers. The clay is well dispersed in PLA/PCL matrix which indicated a mixture of intercalated type nanocomposites which agree with the result of XRD as large increase of basal spacing of the clay layers. Therefore, good surface contact between polymer and clay as the complete dispersal of reinforcing phase in composites [15].

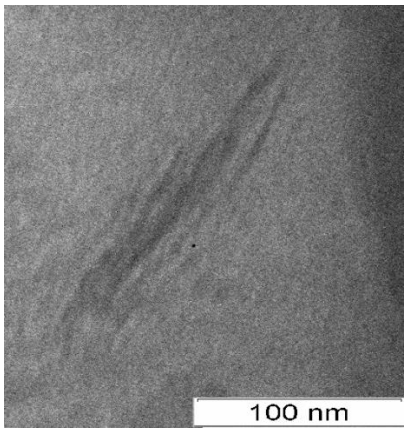

Figure 3: TEM micrographs of PLA/PCL/ 1 wt% clay

3.1.4 Tensile Properties

The tensile strength of PLA/PCL/clay nanocomposites is shown in Figure 4. When 1% of clay added into the blends, the tensile strength increase about 16.89% (53.703 MPa) respectively compared to the unfilled PLA/PCL blends (45.943 MPa). On the other hands, when higher amount of clay added into the blends, the tensile strength decrease gradually. Incorporation of clay increase interfacial adhesion which improves stress transfer within nanocomposites and then cause tensile strength to increase [16]. However, further increase the clay content decrease the tensile strength as the excess clay is dispersed in the matrix which cause formation of agglomeration [17].

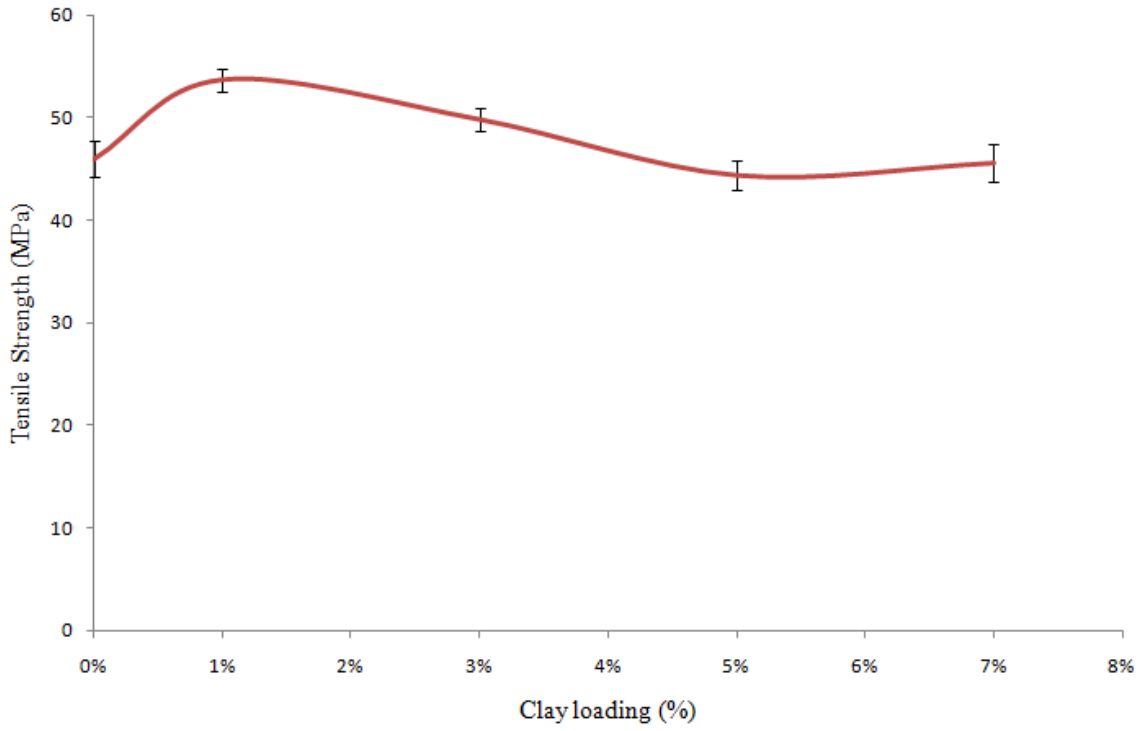

Figure 4: Tensile strength of PLA/PCL/clay nanocomposites

Figure 5 shows the effect of clay loading on the tensile modulus of PLA/PCL blends. The tensile modulus of PLA/PCL blends increases from 902.925 MPa to 906.233 MPa when 1wt% clay is added. The tensile modulus decreases when higher amount of clay is added. As

high aspect ratio of clay (1 wt%), the surface area exposed to the polymer is huge and the region of the polymer matrix is physisorbed on the silicate surface, thus stiffened through its affinity for and adhesion on the filler surfaces [18].

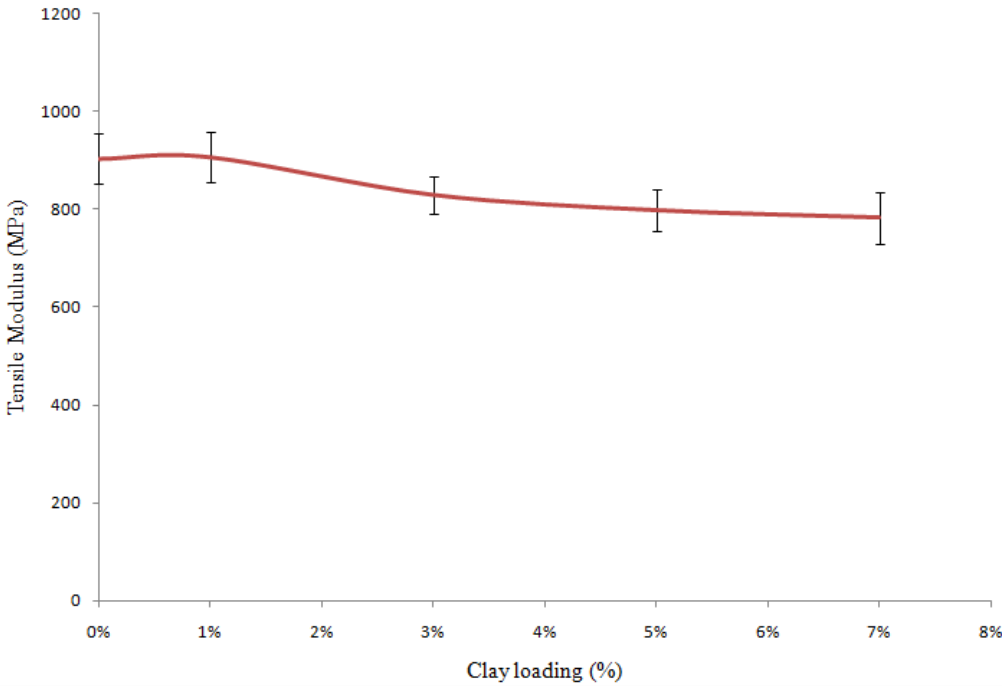

Figure 5: Tensile Modulus of PLA/PCL/clay nanocomposites

The relation between elongation at break and clay loading is illustrated in Figure 6. The addition of 1% clay significantly increases the elongation at break of PLA/PCL blends from 1.679 mm to 4.847 mm with the increment around 188.68%. When higher amount of clay added into the blends, the elongation at break decreases. This might due to existence of large agglomerates which makes nanocomposites become more brittle.

Therefore, 1% of clay will add into PLA/PCL/OPMF biocomposites to investigate effect of clay to biocomposites as it enhances most to the PLA/PCL blends.

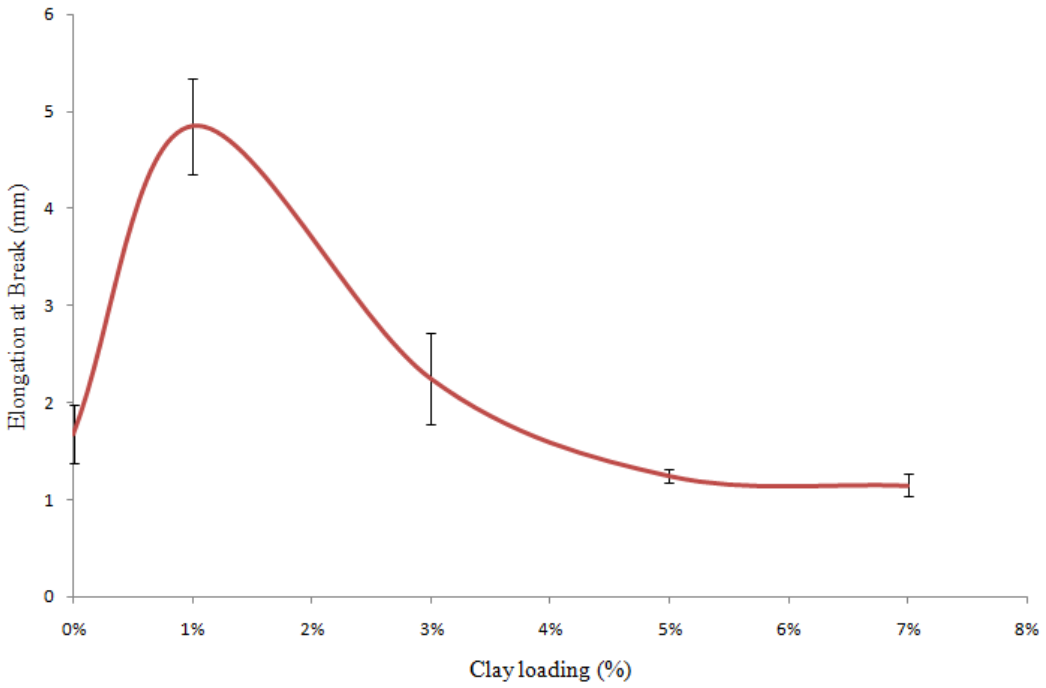

Figure 6: Elongation at Break of PLA/PCL/clay nanocomposites

3.2 PLA/PCL/OPMF/Clay Bionanocomposites Fourier Transform Infrared Spectroscopy (FTIR)

FTIR spectra of PLA/PCL/OPMF biocomposites and PLA/PCL/OPMF/ 1 wt% clay bionanocomposites are shown in Figure 7. Both composites exhibits strong absorbance peak at 1748.90 cm^{-1} and 1745.54 cm^{-1} respectively indicated the presence of C=O stretching. C-H stretching present in both composites but the intensity of PLA/PCL/OPMF/clay bionanocomposites (2939.83 cm^{-1}) is higher than PLA/PCL/OPMF biocomposites (2947.02 cm^{-1}). PLA/PCL/OPMF/clay bionanocomposites consist of peak at 3272.76 cm^{-1} indicated the presence of hydrophilic clay in composites.

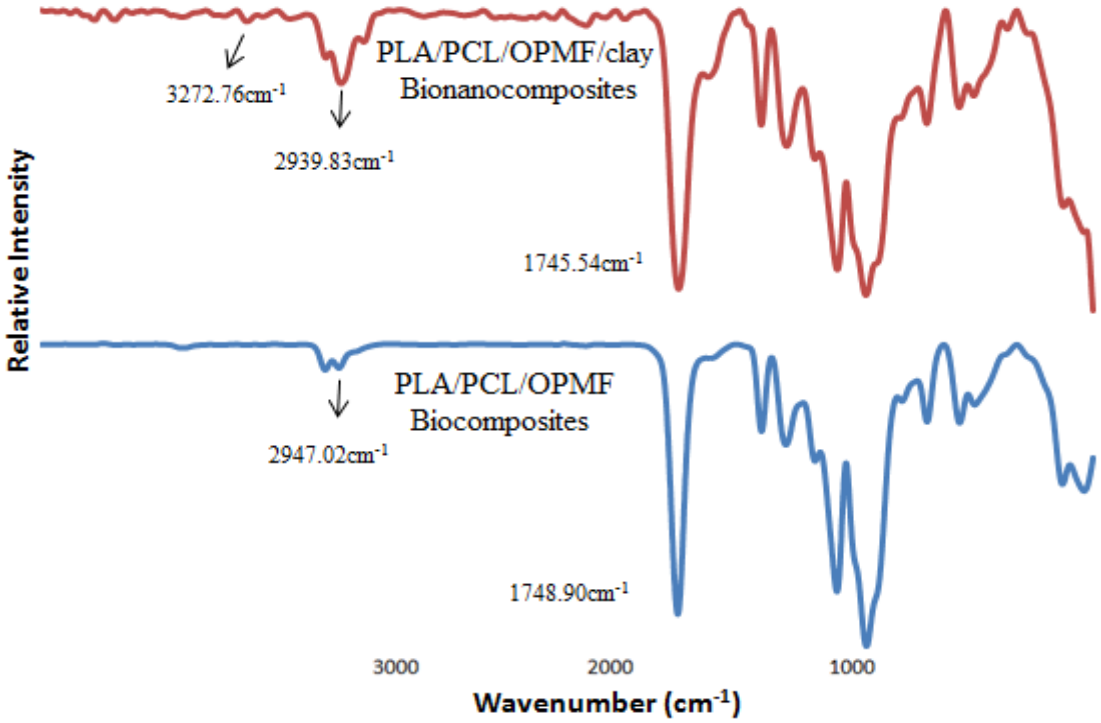

Figure 7: FTIR spectra of PLA/PCL/OPMF biocomposites and PLA/PCL/OPMF/Clay bionanocomposites

3.2.1 Tensile Properties

Figure 8 shows tensile strength of PLA/PCL/OPMF biocomposites and PLA/PCL/OPMF/1 wt% clay bionanocomposites. PLA/PCL/OPMF biocomposites show maximum tensile strength at 10% of the filler content (33.478 MPa) and decrease with the increasing of filler loading which due to poor dispersion causes agglomeration of fillers. Besides, fiber acts as included filler in the resin matrix, which actually weakens the composite because of the poor interfacial adhesion and obstructs the stress propagation, causes the tensile strength to decrease as the filler loading increases [19]. However, the presence of hydrophilic nanoclay increase the overall tensile strength of bionanocomposites and show maximum tensile strength at 10% of the filler content (36.32 MPa) which suggest that the presence of hydrophilic nanoclay act as compatibilizing agents between hydrophilic

fiber and hydrophobic matrix and thus improve the fiber/matrix adhesion of bionanocomposites.

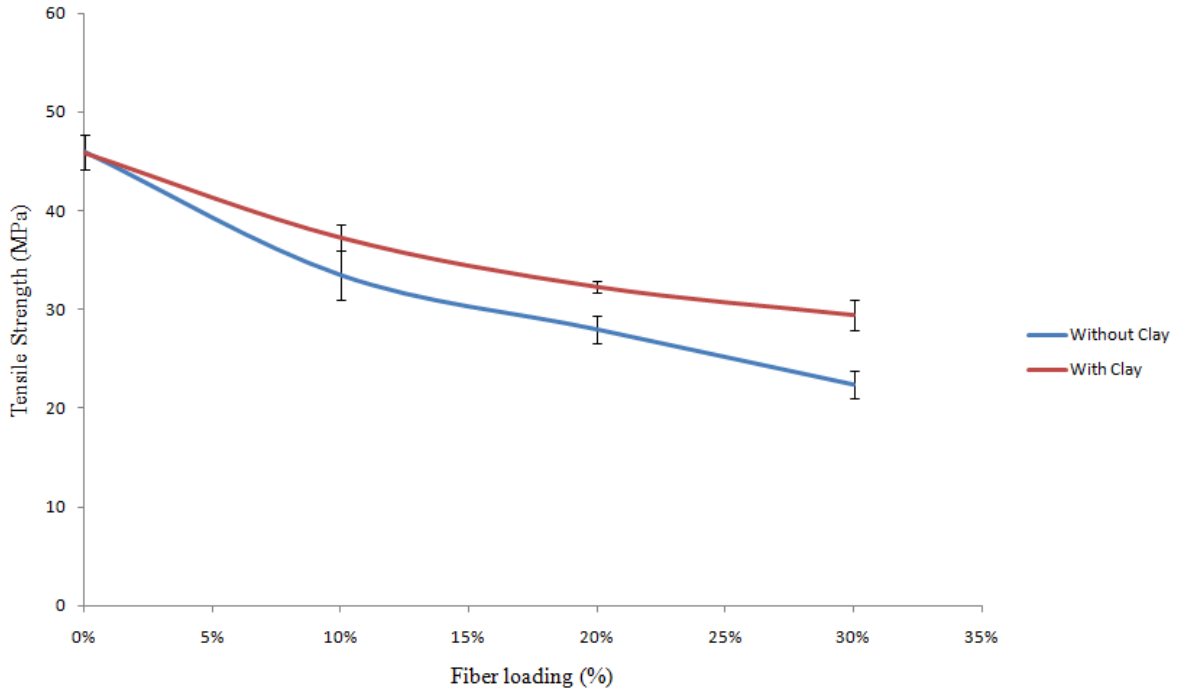

Figure 8: Tensile strength of PLA/PCL/OPMF biocomposites and PLA/PCL/OPMF/Clay bionanocomposites

Tensile modulus of PLA/PCL/OPMF biocomposites and PLA/PCL/OPMF/1 wt% clay bionanocomposites were illustrated in figure 9. PLA/PCL/OPMF biocomposites and PLA/PCL/OPMF/clay bionanocomposites shows highest tensile modulus at 10% of fiber loading which are 884.8 MPa and 685.8 MPa respectively. The overall tensile modulus of biocomposites higher than bionanocomposites. Therefore, the addition of hydrophilic nanoclay decreases the stiffness of the bionanocomposites as the flexibility of composites increase which leads to lower tensile modulus.

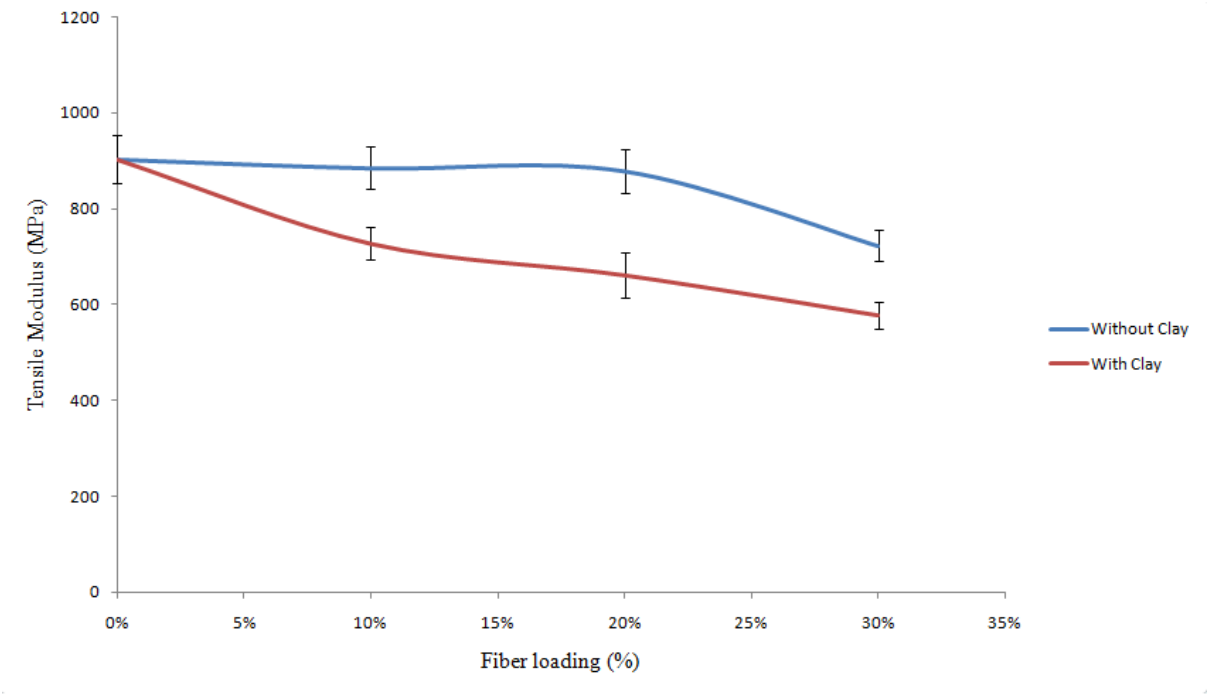

Figure 9: Tensile modulus of PLA/PCL/OPMF biocomposites and PLA/PCL/OPMF/Clay bionanocomposites

Figure 10 illustrated elongation at break PLA/PCL/OPMF biocomposites and PLA/PCL/OPMF/1 wt% clay bionanocomposites. The addition of fiber decrease the elongation at break of composites from 1.679 mm to 0.56 mm (PLA/PCL/OPMF biocomposites) and 0.74 mm (PLA/PCL/OPMF/1 wt% clay bionanocomposites) respectively. This is due to addition of fiber into matrix cause composites to become stiffer and harder as the segment mobility of the composites is reduced. On the other hand, the addition of hydrophilic nanoclay improves the fiber/matrix adhesion of bionanocomposites and also stress transfer within bionanocomposites which enhance the flexibility of the composites. Therefore, PLA/PCL/OPMF/1 wt% clay bionanocomposites shows better elongation at break than PLA/PCL/OPMF biocomposites.

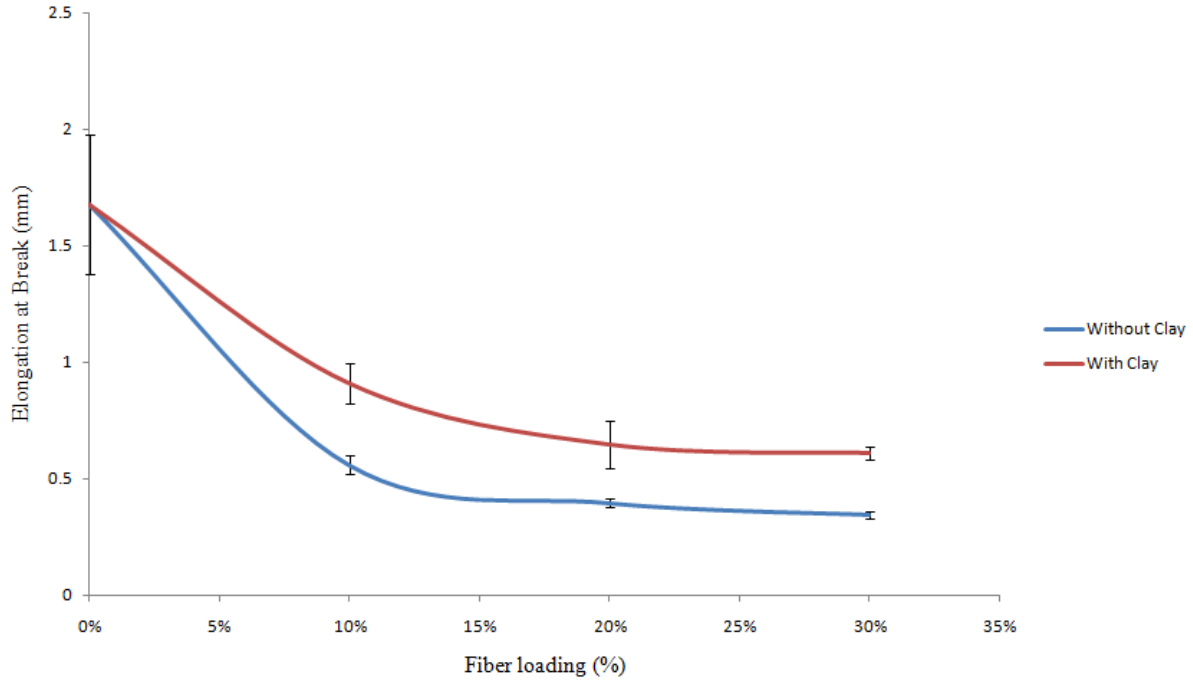

Figure 10: Elongation at break of PLA/PCL/OPMF biocomposites and PLA/PCL/OPMF/Clay bionanocomposites

3.2.2 Themogravimetric Analysis (TGA)

Figure 11 and 12 show TGA and DTG thermogram of PLA/PCL/OPMF biocomposites and PLA/PCL/OPMF/1 wt% clay bionanocomposites. The weight loss of the composites due to degradation is monitored as a function of temperature. The PLA/PCL/OPMF biocomposites show onset temperature of 196.01°C, which increase to 221.12°C when hydrophilic nanoclay is added into the biocomposites. The incorporation of clay into the biocomposites enhances the thermal stability. This is due to clay can hinder the permeability of volatile degradation products out of the materials. The dispersed clay generates a barrier which delays the release of thermal degradation products in comparison the pristine polymer [20].

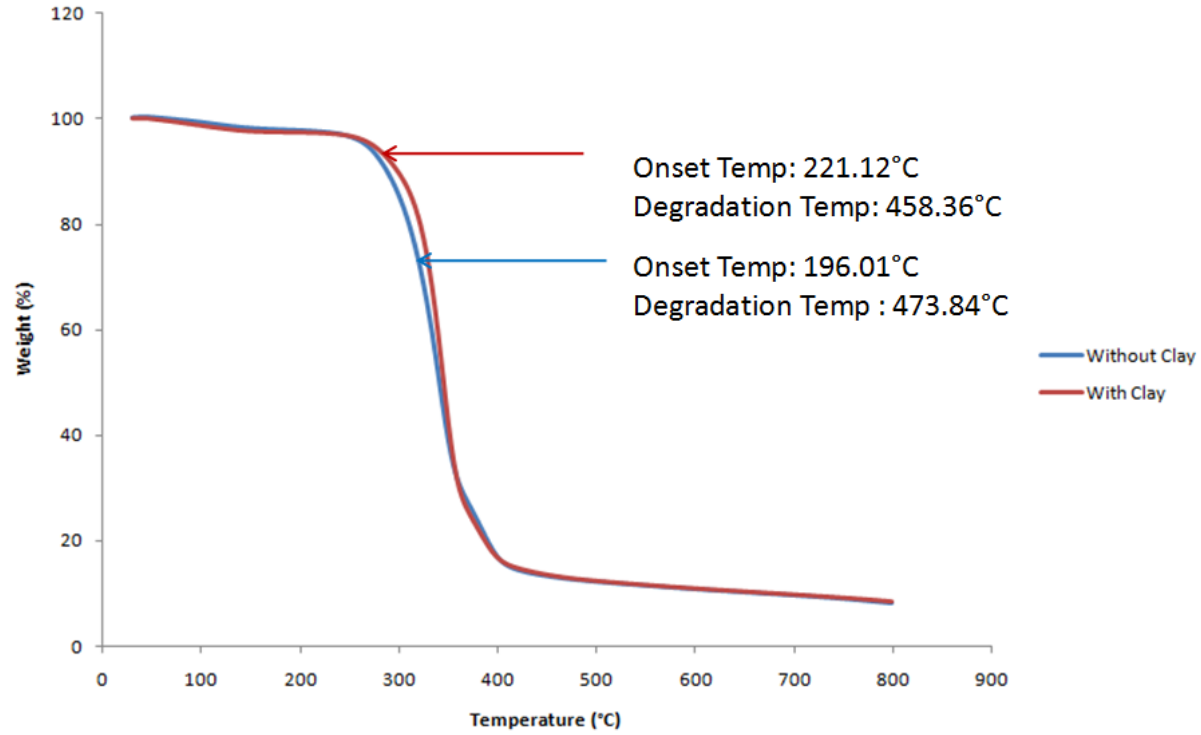

Figure 11: TGA thermogram of PLA/PCL/OPMF biocomposites and PLA/PCL/OPMF/Clay bionanocomposites

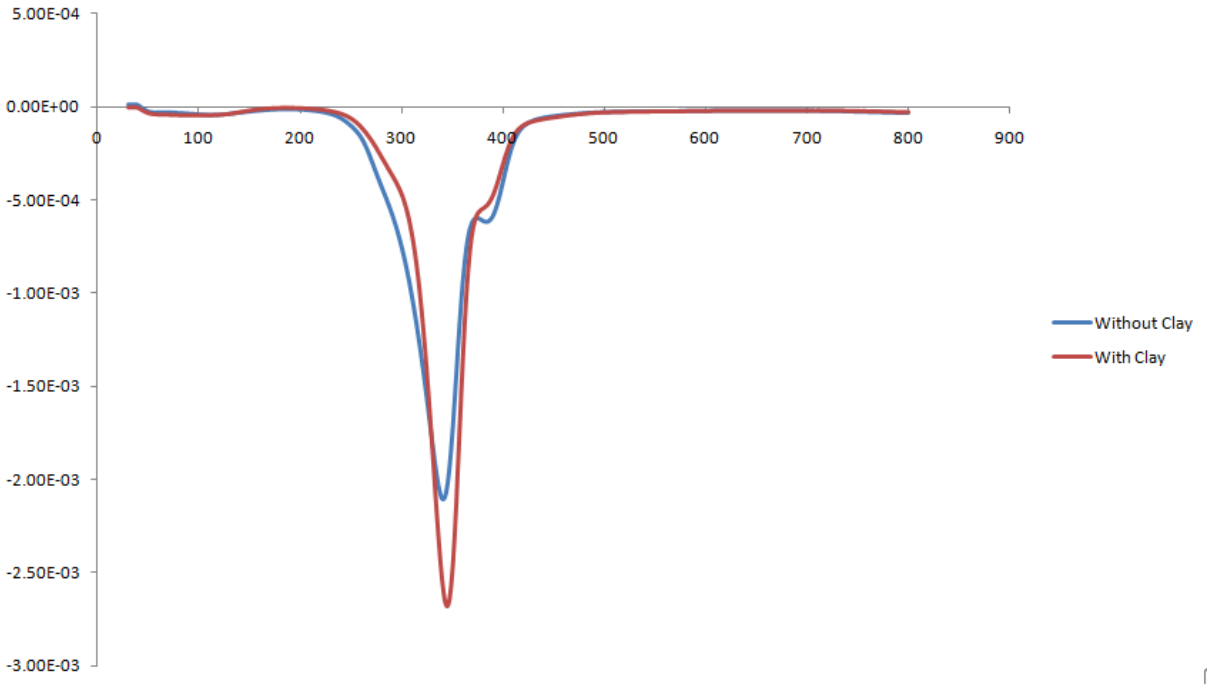

Figure 12: DTG thermogram of PLA/PCL/OPMF biocomposites and PLA/PCL/OPMF/Clay bionanocomposites

3.2.3 Scanning Electron Microscopy (SEM)

SEM micrograph of fractured surface of (a) PLA/PCL/OPMF biocomposites and (b) PLA/PCL/OPMF/1 wt% clay bionanocomposites are shown in Figure 13 at magnification of 150X. Figure 13a shows that PLA/PCL/OPMF biocomposites consists of cavity as fiber been pulled out from matrix indicated poor fiber/matrix adhesion as fiber could not provide an efficient stress transfer from the matrix to the filler causing them to have lower mechanical properties in response to stress. PLA/PCL/OPMF/1 wt% clay bionanocomposites (Figure 13b) shows better fiber/matrix adhesion as no cavity present and fiber-breakage could be seen on facture surfaces indicating better fiber matrix adhesion which is in agreement with the mechanical properties results.

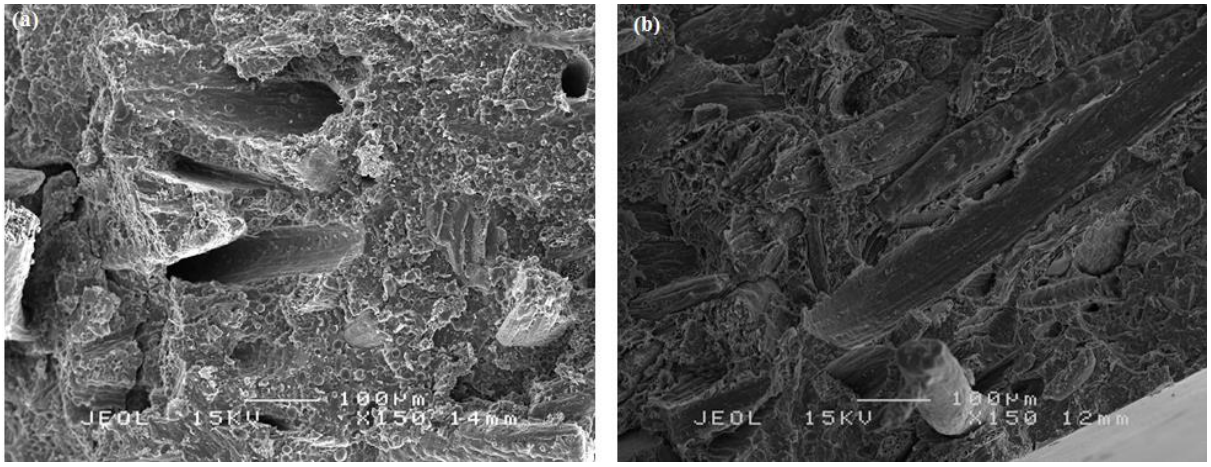

Figure 13: SEM micrograph of (a) PLA/PCL/OPMF biocomposites and (b) PLA/PCL/OPMF/clay bionanocomposites

4.0 CONCLUSION

The addition of hydrophilic nanoclay successfully enhances morphology, mechanical and thermal properties of PLA/PCL/OPMF biocomposites. FT-IR spectra indicated no major peak shifting or formation of new peak in the composites spectra. XRD and TEM results supported intercalated types of PLA/PCL/clay nanocomposites was formed.

PLA/PCL/OPMF/1 wt% clay bionanocomposites shows better tensile strength and elongation at break than PLA/PCL/OPMF biocomposites. The presence of 1 wt% clay increases the thermal stability of the bionanocomposites which shown by TGA thermogram. SEM micrographs revealed that PLA/PCL/OPMF biocomposites consists of cavity as fiber been pulled out which indicated poor fiber/matrix adhesion while micrographs of PLA/PCL/OPMF/1 wt% clay bionanocomposites shows better fiber/matrix adhesion as no cavity present fiber-breakage could be seen at facture surfaces .

ACKNOWLEDGEMENT

The authors would like to thank the Research University Grant Scheme **(**RUGS**),** UPM for their financial support. All the technical staffs in the Department of Chemistry, Faculty of Science, Universiti Putra Malaysia are greatly acknowledged for their assistance.

CONFLICT OF INTEREST

The authors declare that there is no conflict of interest with any financial organization regarding the materials discussed in the manuscript.

REFERENCES

1. M.A.A Mohammed, A. Salmiaton, W.A.K.G Wan Azlina, M.S Mohammad Amran, A. Fakhru'l-Razi, Y.H. Taufiq-Yap. Hydrogen rich gas from oil palm biomass as a potential source of renewable energy in Malaysia. Renewable and Sustainable Energy Reviews 2011, 15 (2): 1258-1270.
2. W.P.Q Ng, H.L Lam, F.Y Ng, M. Kamal, J.H.E Lim. Waste-to-wealth: green potential from palm biomass in Malaysia. Journal of Cleaner Production 2012, 34 (0): 57-65.
3. H. Lik Nang Lau, Y.M. Choo, A.N Ma, C.H Chuah. Selective extraction of palm carotene and vitamin E from fresh palm-pressed mesocarp fiber (Elaeis guineensis) using supercritical CO2. Journal of Food Engineering 2008, 84 (2): 289-296.
4. S.H. Lim, A.S Baharuddin, M.N Ahmad, U.K. Md Shah, N.A Abdul Rahman, S. Abd-Aziz, M.A Hassan, Y. Shirai. Physicochemical Changes in Windrow Co-Composting Process of Oil Palm Mesocarp Fiber and Palm Oil Mill Effluent

Anaerobic Sludge. Australian Journal of Basic and Applied Sciences 2009, 3 (3): 2809-2816.
5. Sreekala, M. S.; Kumaran, M. G.; Thomas, S., Oil palm fibers: Morphology, chemical composition, surface modification, and mechanical properties. Journal of Applied Polymer Science 1997, 66 (5), 821-835.
6. P. Wambua, J. Ivens, I. Verpoest. Natural fibres: can they replace glass in fibre reinforced plastics? Composites Science and Technology 2003, 63 (9): 1259-1264.
7. J.E Riccieri, A. Vázquez, L.H. De Carvalho. Interfacial properties and initial step of the water sorption in unidirectional unsaturated polyester/vegetable fiber composites. Polymer Composites 1999, 20 (1): 29-37.
8. N.A. Ibrahim, W.M.Z.W Yunus, O. Maizatulnisa, A. Khalina, K.A Hadithon. Poly(Lactic Acid) (PLA)-reinforced Kenaf Bast Fiber Composites: The Effect of Triacetin. Journal of Reinforced Plastics and Composites 2010, 29 (7): 1099-1111.
9. H. Balakrishnan, A. Hassan, M.U Wahit, A.A Yussuf, S.B.A Razak. Novel toughened polylactic acid nanocomposite: Mechanical, thermal and morphological properties. Materials & Design 2010, 31 (7): 3289-3298.
10. J.T Yeh, C.J Wu, C.H Tsou,W.L Chai, J.D Chow, C.Y Huang, K.N Chen, C.S Wu. Study on the Crystallization, Miscibility, Morphology, Properties of Poly(lactic acid)/Poly(ε-caprolactone) Blends. Polymer-Plastics Technology and Engineering 2009, 48 (6): 571-578.
11. W.H Hoidy, M.B Ahmad, E.A Jaffar Al-Mulia, N.A Ibrahim. Preparation and Characterization of Polylactic Acid/Polycaprolactone Clay Nanocomposites. Journal of Applied Sciences 2010, 10: 97-106.
12. M. Darder, P. Aranda, E. Ruiz-Hitzky. Bionanocomposites: A New Concept of Ecological, Bioinspired, and Functional Hybrid Materials. Advanced Materials 2007**,** 19 (10): 1309-1319.
13. B. Kord. Nanofiller reinforcement effects on the thermal, dynamic mechanical and morphological behavior of HDPE/rice husk flour composites. Bioresources 2011, 6 (2): 1351-1358.
14. J. Madejova, P. Komadel. Baseline studies of the clay minerals society source clays: Infrafed Methods. Clays and Clay Minerals 2001, 49 (5): 410-432.
15. N.A Ibrahim, B.W Chieng, W.M.Z.W Yunus. Morphology, Thermal and Mechanical Properties of Biodegradable Poly(butylene succinate)/Poly(butylene adipate-co-terephthalate)/Clay Nanocomposites. Polymer-Plastics Technology and Engineering 2010, 49 (15): 1571-1580.
16. H. Essawy, D. El-Nashar. The use of montmorillonite as a reinforcing and compatibilizing filler for NBR/SBR rubber blend. Polymer Testing 2004, 23: 803-807.
17. S.N. Sathe, G.S Srinivasa Rao, K.V Rao, S. Devi. The effect of composition on morphological, thermal, and mechanical properties of polypropylene/nylon-6/polypropylene-g-butyl acrylate blends. Polymer Engineering and Science 1996, 36 (19): 2443-2450.
18. Z. Yu, J. Yin, S. Yan, Y. Xie, J. Ma, X. Chen. Biodegradable poly(l-lactide)/poly(ε-caprolactone)-modified montmorillonite nanocomposites: Preparation and characterization. Polymer 2007, 48 (21): 6439-6447.
19. H.S Yang, H.J Kim, H.J Park, B.J Lee, T.S Hwang. Water absorption behavior and mechanical properties of lignocellulosic filler–polyolefin bio-composites. Composite Structures 2006, 72 (4): 429-437.
20. T. Agag, T. Koga, T. Takeichi. Studies on thermal and mechanical properties of polyimide–clay nanocomposites. Polymer 2001, 42 (8): 3399-3408.